Quantum Enhanced Cavity QED Interferometer with Partially Delocalized Atoms in Lattices

Anjun Chu,[1,2,*] Peiru He,[1,2] James K. Thompson,[1] and Ana Maria Rey[1,2]
[1]JILA, NIST and Department of Physics, University of Colorado, Boulder, Colorado 80309, USA
[2]Center for Theory of Quantum Matter, University of Colorado, Boulder, Colorado 80309, USA

(Received 15 April 2021; accepted 12 October 2021; published 17 November 2021)

We propose a quantum enhanced interferometric protocol for gravimetry and force sensing using cold atoms in an optical lattice supported by a standing-wave cavity. By loading the atoms in partially delocalized Wannier-Stark states, it is possible to cancel the undesirable inhomogeneities arising from the mismatch between the lattice and cavity fields and to generate spin squeezed states via a uniform one-axis twisting model. The quantum enhanced sensitivity of the states is combined with the subsequent application of a compound pulse sequence that allows us to separate atoms by several lattice sites. This, together with the capability to load small atomic clouds in the lattice at micrometric distances from a surface, make our setup ideal for sensing short-range forces. We show that for arrays of 10^4 atoms, our protocol can reduce the required averaging time by a factor of 10 compared to unentangled lattice-based interferometers after accounting for primary sources of decoherence.

DOI: 10.1103/PhysRevLett.127.210401

Introduction.—Ultracold atomic systems offer tremendous potential for quantum sensing applications including time keeping [1] and gravimetry [2], and thus provide opportunities for searching or constraining new physics in outstandingly precise and compact experiments. Despite the great advances in quantum sensing accomplished by cold atom experiments, one of the most important milestones that needs to be accomplished is to introduce quantum entanglement to enhance the sensitivity of real-world sensors beyond the so-called standard quantum limit (SQL) attainable with uncorrelated particles [3–6].

Important steps towards this goal have been accomplished such as the generation of up to 19 dB spin squeezing in cavities [7–10]. Nevertheless, the use of entangled states in state-of-the-art inertial sensors has yet to be achieved. Limitations include the spatial mismatch between the lattice potential and the cavity mode which degrades the utility of spin squeezing after releasing the atomic cloud to free space [11]. Conventional free-falling experiments also lack spatial resolution and suffer from limited interrogation time [12]. Theoretical and experimental progress to overcome these challenges has been reported in recent years although in different setups. For example, homogeneous atom-cavity couplings have been engineered by the use of commensurate lattices [7,13,14], ring cavities [15–18], or via time averaging as atoms free fall along the cavity axis [19]. In parallel, lattice-based interferometers enjoying compact spatial volumes [12,20–23] have reported capabilities to trap atoms near surfaces, and have achieved up to 20 s holding time using uncorrelated atoms [22].

Here we propose a quantum enhanced lattice-based protocol that uses the motional eigenstates of the combined lattice plus gravity potential, the so-called Wannier-Stark (WS) states, to overcome relevant limitations faced by current atomic sensors. The key idea is the use of delocalized WS states over a few lattice sites, which enables averaging out the inhomegeneities of atom-cavity couplings at specific lattice depths. This allows for the generation of uniform spin squeezed states via dynamical one-axis twisting (OAT) evolution [24,25], or via homogeneous quantum nondemolition (QND) measurements [26,27], even in incommensurate lattice-cavity geometries. The uniformly generated spin squeezed states are not only useful for quantum enhanced measurements of gravity [14], but also ideal for fundamental tests of short-ranged forces [12,22] which require loading small atomic clouds close to a surface or a source mass, such as dark energy [28], Casimir-Polder forces [29], and non-Newtonian corrections of gravity [30,31]. Furthermore, the ability to tune the inhomogeneities of couplings to a bosonic mode that mediates interactions or introduces disorder opens new possibilities in quantum many-body simulators [32].

Our work focuses on the dynamical generation of spin squeezing and the interferometric sequence to transfer the atoms to WS orbitals separated by several lattice sites to improve phase accumulation. Moreover, the interferometric phase can be mapped into a magnified rotation of the atomic internal state by reversing the squeezing protocol, which can be measured without the need of below-SQL detection resolution [33–35]. After accounting for primary sources of decoherence, we show that applying our scheme

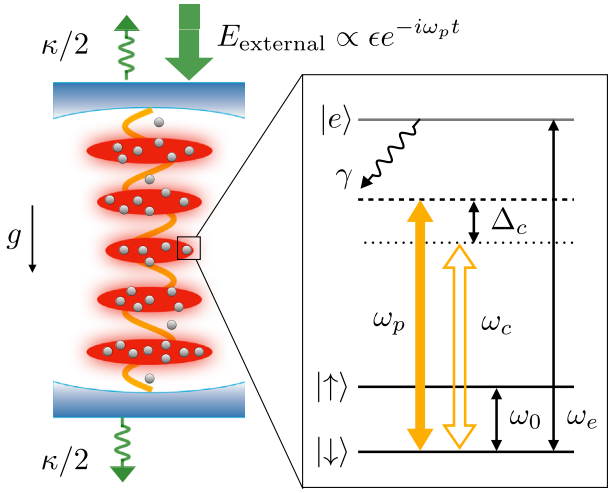

FIG. 1. Protocol schematics: An ensemble of ultracold atoms are trapped in the lowest band of a lattice supported by a standing-wave optical cavity oriented along the direction of the gravitational acceleration g. The cavity decay rate is $\kappa/2$ on each side. The two long-lived internal levels of an atom with energy splitting $\hbar\omega_0$ act as a spin-1/2 degree of freedom labeled as $|\uparrow\rangle$ and $|\downarrow\rangle$. These two states are coupled through a single cavity mode to the excited state $|e\rangle$, with energy $\hbar\omega_e$ and spontaneous emission rate γ. The cavity mode is coherently pumped by an external light field with detuning $\Delta_c = \omega_p - \omega_c$ from the cavity resonance which generates a net injected field in the cavity with amplitude ϵ.

to arrays of 10^4 atoms, it should be possible to detect short-range forces acting at μm-scale distances, with an averaging time reduced by a factor of 10 compared to unentangled lattice-based interferometers [12,20].

System.—We consider an ensemble of N ultracold atoms, with mass M trapped in a vertical standing-wave optical cavity, as depicted in Fig. 1. The atoms are confined in the lowest band of a one-dimensional (1D) optical lattice oriented along the vertical direction $\hat{z}$. The gravitational potential with local acceleration g generates a differential energy shift Mgz between two atoms separated by a vertical distance z. Two long-lived internal levels of the atoms, with energy splitting $\hbar\omega_0$, are used to encode a spin-1/2 degree of freedom with states labeled as $|\uparrow\rangle$ and $|\downarrow\rangle$. A single cavity mode with frequency ω_c and wavelength λ_c couples the $|\uparrow\rangle$ and $|\downarrow\rangle$ states to an optically excited state $|e\rangle$ of the atoms separated by a frequency ω_e from the $|\downarrow\rangle$ state. The atom-cavity coupling has a spatial profile $\mathcal{G}_{\uparrow,\downarrow}(z) = \mathcal{G}^0_{\uparrow,\downarrow}\cos(k_c z)$, where $k_c = 2\pi/\lambda_c$. The cavity mode is coherently pumped by an external field detuned from the cavity resonance by $\Delta_c = \omega_p - \omega_c$.

We are focusing on the system operating in the dispersive regime of atom-light interaction, where both the pump and cavity mode are far detuned from the atomic resonances, i.e., $\Delta_{\uparrow,\downarrow} \gg \mathcal{G}^0_{\uparrow,\downarrow}\sqrt{\langle\hat{a}^\dagger\hat{a}\rangle}$, with $\Delta_\uparrow = \omega_p - \omega_e + \omega_0$ and $\Delta_\downarrow = \omega_p - \omega_e$. In this limit, the atomic excited state $|e\rangle$ can be adiabatically eliminated [36], leading to the following Hamiltonian written in second quantized form in the rotating frame of the external optical pumping field,

$$\hat{H} = \sum_{\beta=\uparrow,\downarrow}\int dz\hat{\psi}^\dagger_\beta(z)\left[\frac{\hat{p}^2}{2M} + V_0\sin^2(k_l z) + Mgz + \frac{\hbar|\mathcal{G}_\beta(z)|^2}{\Delta_\beta}\hat{a}^\dagger\hat{a}\right]\hat{\psi}_\beta(z) + \hat{H}_{\text{cav}} + \hat{H}_{\text{drive}}. \quad (1)$$

Here, V_0 is the lattice depth, $k_l = 2\pi/\lambda_l$ is the wave number of lattice beams that sets the atomic recoil energy $E_R = \hbar^2 k_l^2/2M$ and the lattice spacing $a_l = \lambda_l/2$, where λ_l is the wavelength of the lattice. The operator $\hat{a}$ is the annihilation field operator for cavity photons, and the operator $\hat{\psi}_\beta(z)$ annihilates an atom of spin β at position z. The cavity Hamiltonian is given by $\hat{H}_{\text{cav}}/\hbar = -\Delta_c\hat{a}^\dagger\hat{a} + \epsilon\hat{a}^\dagger + \epsilon^*\hat{a}$, where ϵ is the amplitude of the injected field. The drive Hamiltonian $\hat{H}_{\text{drive}}/\hbar = \int dz\{[\Omega\hat{\psi}^\dagger_\uparrow(z)\hat{\psi}_\downarrow(z) + \text{H.c.}] - \delta\hat{\psi}^\dagger_\uparrow(z)\hat{\psi}_\uparrow(z)\}$ describes a switchable external microwave drive, with Rabi frequency Ω, drive detuning δ that uniformly couples the spin-1/2 degree of freedom when applied.

We expand the atom field operators $\hat{\psi}_\beta(z)$ in terms of the Wannier-Stark (WS) orbitals: $\hat{\psi}_\beta(z) = \sum_n \hat{c}_{n\beta}\phi_n(z)$, where $\hat{c}_{n\beta}$ annihilates an atom of spin β in the WS state $|\phi_n\rangle$ centered at site n. In the tight-binding limit, the wave function of the WS state $|\phi_n\rangle$ takes the form $\phi_n(z) = \sum_m \mathcal{J}_{m-n}(2J_0/Mga_l)w(z - ma_l)$ [37], where $\mathcal{J}_n(x)$ is the Bessel function of the first kind, $J_0/\hbar$ is the nearest-neighbor tunneling rate, and $w(x)$ is the ground band Wannier function. If we assume the cavity-induced ac Stark shifts $\hbar|\mathcal{G}^0_{\uparrow,\downarrow}|^2\langle\hat{a}^\dagger\hat{a}\rangle/\Delta_{\uparrow,\downarrow}$ are smaller than Mga_l [36], so transitions between WS orbitals are suppressed, the atom-cavity dynamics can be simplified into the following Hamiltonian,

$$\hat{H} = \hbar\sum_n(-\delta + \eta_n\hat{a}^\dagger\hat{a})\hat{S}^z_n + H_{\text{cav}} + \hbar\sum_n\Omega\hat{S}^x_n. \quad (2)$$

Here, the spin operators are defined in terms of atomic creation and annihilation operators for $|\uparrow_n\rangle \equiv |\uparrow;\phi_n\rangle$ and $|\downarrow_n\rangle \equiv |\downarrow;\phi_n\rangle$ states, $\hat{S}^{x,y,z}_n = \sum_{\beta,\beta'}\hat{c}^\dagger_{n\beta}\sigma^{x,y,z}_{\beta\beta'}\hat{c}_{n\beta'}$, where $\sigma^{x,y,z}_{\beta\beta'}$ are the matrix elements of the corresponding Pauli matrices and $\beta,\beta' \in \{\uparrow,\downarrow\}$. It is also convenient to define the collective spin operators $\hat{S}^{x,y,z} = \sum_n \hat{S}^{x,y,z}_n$ for later discussions. The dispersive atom-light coupling $\eta_n = \eta^\uparrow_n - \eta^\downarrow_n$, with $\eta^{\uparrow,\downarrow}_n = \int dz|\mathcal{G}_{\uparrow,\downarrow}(z)\phi_n(z)|^2/\Delta_{\uparrow,\downarrow}$, can be evaluated analytically,

$$\eta_n = \eta\left[1 + \mathcal{C}\mathcal{J}_0\left(\frac{4J_0}{Mga_l}\sin(\varphi/2)\right)\cos(n\varphi)\right], \quad (3)$$

where $\eta = \frac{1}{2}(|\mathcal{G}_{\uparrow}^{0}|^2/\Delta_{\uparrow} - |\mathcal{G}_{\downarrow}^{0}|^2/\Delta_{\downarrow})$ is the mean value of η_n over all possible n, $\varphi = 2\pi\lambda_l/\lambda_c$, and $\mathcal{C}$ is a parameter of order one [36]. We also replace Δ_c by an effective cavity detuning $\tilde{\Delta}_c = \Delta_c - \sum_n N_n(\eta_n^{\uparrow} + \eta_n^{\downarrow})/2$ in $\hat{H}_{\rm cav}$, where N_n is the total atom number in $|\uparrow_n\rangle$ and $|\downarrow_n\rangle$ states.

The last step is to adiabatically eliminate the injected light field and intracavity fluctuations, possible in the limits $\tilde{\Delta}_c \gg \eta\alpha\sqrt{N}, \kappa$ [36], where $\alpha = \varepsilon/(\tilde{\Delta}_c + i\kappa/2)$ is the steady-state value of the cavity field, and κ is the cavity intensity decay rate. With these reasonable approximations, the system can well described by an effective Hamiltonian involving only the spins,

$$\hat{H}_{\rm eff}/\hbar = -\sum_n(\delta - \eta_n|\alpha|^2)\hat{S}_n^z + \sum_{nm}\chi_{nm}\hat{S}_n^z\hat{S}_m^z + \Omega\sum_n\hat{S}_n^x. \tag{4}$$

When the microwave drive is off, the Hamiltonian above is the so-called one-axis twisting model, with $\chi_{nm} = \eta_n\eta_m|\alpha|^2\tilde{\Delta}_c/(\tilde{\Delta}_c^2 + \kappa^2/4)$ the OAT interaction strength, which is an iconic model for the generation of spin squeezed states [24,25].

Engineering homogeneous couplings.—One limitation of spin squeezing generation protocols with frozen atoms in deep lattices ($J_0 \approx 0$) is the inhomogeneous couplings arising from incommensurate lattice and cavity mode wavelengths ($\varphi \neq \pi j$ with j an integer). However, in a relatively shallow lattice ($V_0 < 10E_R$) where $J_0 \sim Mga_l$, the wave function of WS states can extend over a few adjacent lattice sites [see Fig. 2(a)] due to non-negligible nearest-neighbor tunnel couplings, instead of being localized in a single site. The lattice depth can thus be used as a control knob to vary the extension of the WS and for tuning the inhomogeneitiy of the spin coupling parameters [see Fig. 2(b)]. In particular, at the magic lattice condition,

$$\mathcal{J}_0\left(\frac{4J_0}{Mga_l}\sin(\varphi/2)\right) = 0, \tag{5}$$

we can completely average out the inhomogeneities and obtain uniform couplings in Eq. (4) with $\eta_n = \eta$ and $\chi_{nm} = \chi = \eta^2|\alpha|^2\tilde{\Delta}_c/(\tilde{\Delta}_c^2 + \kappa^2/4)$. This technique is relevant not only for the generation of homogeneous spin squeezing but also for quantum simulation of long-range spin models with tunable inhomogeneity [32]. In practice, the thermal distribution of atoms in the radial direction and the undesirable couplings between axial and radial confinement of the Gaussian beam profile can lead to an imperfect cancellation [see the insets in Fig. 2(b)], which can be highly suppressed by operating at low radial temperature or large radial confinement [36]. For ^{87}Rb atoms with $\lambda_c = 780$ nm (D_2 transition) and $\lambda_l = 532$ nm, the magic lattice depths are around $6.0E_R$ and $2.9E_R$ [see Fig. 2(b)]. For ^{171}Yb atoms with $\lambda_c = 556$ nm ($^1S_0 \rightarrow {}^3P_1$ transition) and $\lambda_l = 413$ nm [46], the magic lattice depth is around $3.2E_R$. The negligible scattering length of ^{171}Yb atoms [47] and their insensitivity to magnetic and electric fields make them ideal for inertial sensing. For the cases above, at the smallest magic lattice depth the WS state spreads within three lattice sites.

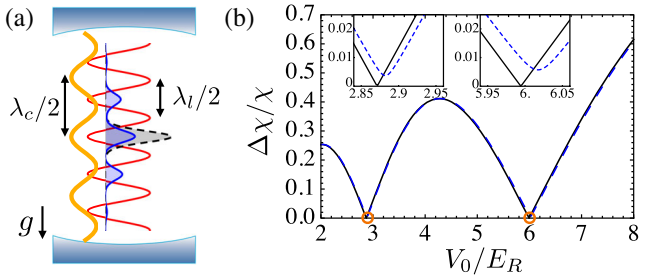

FIG. 2. (a) Inhomogeneous atom-light couplings arise due to the incommensurate wavelengths of the lattice beams (red curve) and the cavity mode (yellow curve), when atoms are frozen in Wannier states (black dashed curve) for deep lattice limit. The inhomogeneities can be cancelled out in a relatively shallow lattice since Wannier-Stark states (blue curve) can extend over a few lattice sites. (b) Standard deviation of the OAT coupling strengths $\Delta\chi = [\sum_{nm}(\chi_{nm} - \chi)^2/N]^{1/2}$ as a function of lattice depth V_0/E_R assuming ^{87}Rb atoms trapped in a $\lambda_l = 532$ nm lattice. The black curve shows the magic lattice depths ($\Delta\chi = 0$) can be achieved around $6.0E_R$ or $2.9E_R$ under ideal conditions, indicated by the orange circles. The blue dashed curve shows the imperfect cancellation of inhomogeneities in χ_{nm} with radial temperature $T = 1$ μK and radial trapping frequency $\omega_r/2\pi = 1$ kHz. The two insets show the zoomed $\Delta\chi/\chi$ near the magic lattice depths.

Quantum enhanced interferometric protocol.—Since the energy splitting of WS states is proportional to the gravitational acceleration g, our system can be directly used for quantum enhanced gravimetry. The protocol consists of the following steps, as illustrated in Fig. 3. After the application of a short $\pi/2$ pulse with the microwave drive in an empty cavity [see Eq. (4) with $\alpha = 0$] that prepares a spin coherent state along $\hat{x}$ direction, the system is let to evolve for a time t_0 under the OAT interaction mediated by the optical cavity [see Eq. (4) with $\Omega = 0$ using an additional spin echo π pulse at $t_0/2$ to cancel additional $\hat{S}^z$ rotations], which results in the generation of a uniform spin squeezed state [see Fig. 3(a)]. The reduced noise quadrature of the state makes it highly sensitive to small rotations about the $\hat{y}$ axis, $\tilde{R}_y^{\phi} = e^{-i\phi\hat{S}^y}$.

To perform precise measurement of a phase ϕ arising from gravitational energy shifts, Raman sideband transitions to WS states separated by a few lattice sites are used. Explicitly, the rotation about the $\hat{y}$ axis is implemented as $\tilde{R}_y^{\phi} = \tilde{R}_x^{-\pi/2}\bar{R}_z^{\phi}\tilde{R}_x^{\pi/2}$, with $\bar{R}_z^{\phi} = (\mathcal{R}^{\dagger})^{m_R}R_z^{\phi}\mathcal{R}^{m_R}$, where m_R is the number of imposed compound pulses, and $\mathcal{R} = \tilde{R}_y^{\pi}R_y^{\pi}$ is a compound pulse to separate the atoms in $|\uparrow\rangle$ and $|\downarrow\rangle$ states by $2r$ lattice sites: $|\uparrow_n\rangle \rightarrow |\uparrow_{n+r}\rangle$ and $|\downarrow_n\rangle \rightarrow |\downarrow_{n-r}\rangle$. It consists of a π Raman pulse R_y^{π} with

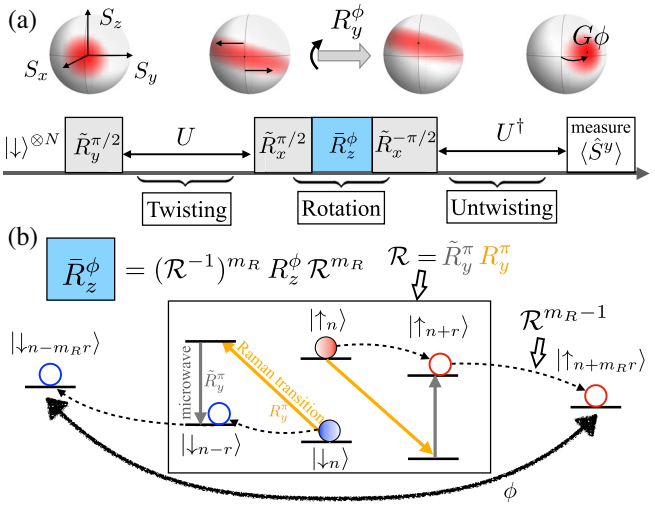

FIG. 3. Schematic of the quantum-enhanced gravimetry using Wannier-Stark (WS) states. (a) After the preparation of a coherent spin state along $\hat{x}$ direction in the carrier transition, we apply the twisting Hamiltonian for a time t_0 as $U = \exp(-i\chi\hat{S}^z\hat{S}^z t_0)$, and the system becomes a squeezed state sensitive to small rotations about the $\hat{y}$ axis ($\tilde{R}_y^\phi$). By applying the untwisting sequence $U^\dagger$ for the same amount of time t_0, the quantum noise returns to the SQL level and the small rotation angle ϕ is amplified into a larger angle $G\phi$ around $\hat{z}$ axis, which can be detected by measuring $\langle\hat{S}^y\rangle$. (b) The phase accumulation due to gravitational energy difference is achieved through a compound pulse sequence that separates the atoms in the corresponding WS states by $2m_Rr$ lattice sites. A single compound pulse $\mathcal{R}$, as shown in the box, is a combination of a microwave pulse in the carrier transition and a Raman pulse for the rth WS sidebands, which generates spin-dependent spatial transfer of the atoms (indicated by red and blue circles) from $|\uparrow_n\rangle/|\downarrow_n\rangle$ to $|\uparrow_{n+r}\rangle/|\downarrow_{n-r}\rangle$.

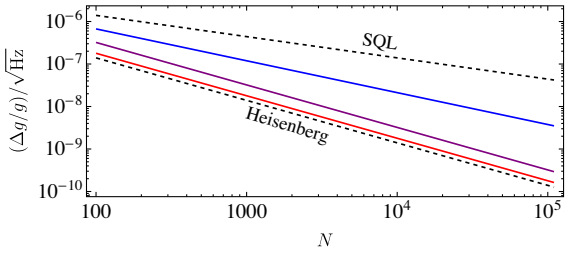

FIG. 4. Interferometer sensitivity $\Delta g/g$ as a function of atom number N, assuming 5.32 μm separation for ^{87}Rb atoms via compound pulse sequence, 1 s phase accumulation time, and $C' = 2$. The red curve indicates the ideal implementation without decoherence, while the blue curve and purple curve take account the effect of cavity loss and spontaneous emission with spin flip probability $P_f = 1/2$ and $P_f = 0$, respectively.

appropriate momentum kick and frequency ω_R to perform the desired r-site transfer in the lattice (apply from side to ensure homogeneity for all atoms), followed by a π pulse on the carrier transition to flip back the spin using a microwave drive ($\tilde{R}_y^\pi$) with frequency ω_{MW} [see Fig. 3(b)]. Such type of compound pulse sequences have been already successfully demonstrated in ^{87}Rb atoms [48]. The R_z^ϕ operator describes the free evolution for a time τ of the atoms separated by $2m_Rr$ lattice sites when they accumulate a phase $\phi = (\omega_{\mathrm{R}} - \omega_{\mathrm{MW}} - Mga_lr/\hbar) \times 2m_R\tau$. Note that one can apply an additional microwave pulse $\tilde{R}_y^\pi$ at $\tau/2$ to remove the undesirable hyperfine energy splitting $\hbar\omega_0$.

Finally, one can perform a time reversal of OAT dynamics by changing the frequency of pump laser such that $\tilde{\Delta}_c \to -\tilde{\Delta}_c$, followed by a measurement of $\langle\hat{S}^y\rangle$ [33]. Under this untwisting sequence, the accumulated phase ϕ is amplified by a factor of $G = (\partial_\phi\langle\hat{S}^y\rangle/S)_{\phi\to 0}$, and the quantum noise for phase measurement $\sigma_p = (\Delta S^y/S)_{\phi\to 0}$ returns to the SQL level, $(\sigma_p)_{\mathrm{SQL}} = 1/\sqrt{N}$, which leads to a phase sensitivity $\Delta\phi = \sigma_p/G$ achievable with detection resolution at the atom shot noise level. So we estimate a sensitivity of gravimetry by $\Delta g/g = \xi/(\phi_g\sqrt{N}) \times \sqrt{\tau/T}$, where $\phi_g = 2Mga_lrm_R\tau/\hbar$, $\xi^{-2} = 1/[N(\Delta\phi)^2]$ is the metrological gain over the SQL, and T is the averaging time. The optimal sensitivity approaches the Heisenberg limit $\Delta g/g \propto 1/N$ under pure Hamiltonian dynamics [see the red curve in Fig. 4].

Our protocol could be also ideal for sensing weak short-range forces generated by an object placed close to the atoms [28–31], which introduces new possibilities in exploring new physics beyond the standard model. Such forces will generate an additional potential $\mathcal{U}(z)$ that will mainly modify the phase accumulated by an atom in the WS state centered at site n to $\tilde{\phi}_n = \phi + (\mathcal{U}_{n+m_Rr} - \mathcal{U}_{n-m_Rr})\tau/\hbar$, where $\mathcal{U}_n = \int dz\mathcal{U}(z)|\phi_n(z)|^2$. Given the dependence of the phase on initial WS states, which will dephase the atomic sample if spreading over multiple WS states, the use of atomic clouds with small spatial extension to reduce the number of occupied WS states can be crucial. For these situations, since the inhomogeneities in atom-light couplings do not average out in a single realization, one needs to account for important systematic errors in the amplification factor G, in contrast to the subdominant suppression of G when the atomic array is fully spread across the lattice [36]. Therefore, the magic lattice condition can lead to significant improvements if the atoms are restricted to local regions of the lattice.

Experimental considerations.—Experimental imperfections such as cavity loss and spontaneous emission of the excited state during the spin squeezing generation and other dephasing mechanisms during the interrogation will degrade the ideal sensitivity in practical implementations as we now discuss. Cavity loss induces phase fluctuations of the collective spin with collective dephasing rate $\Gamma_z = \chi\kappa/\tilde{\Delta}_c$, which lead an increase in the variance of $\hat{S}^y$. Spontaneous emission from the excited state $|e\rangle$, at a rate γ, generates off-resonant photon scattering processes with a total rate $\Gamma \propto \gamma|\mathcal{G}^0_{\uparrow,\downarrow}|^2|\alpha|^2/\Delta^2_{\uparrow,\downarrow}$, including single-particle spin flips and dephasing. Here we focus on the case

with balanced spin flip rates, $\gamma_r = P_f\Gamma$ with P_f the spin flip probability, which can be achieved by choosing appropriate energy levels and detunings, so the spontaneous emission generates no biases on the accumulated phase ϕ. The noise induced by the γ_r terms is amplified during the untwisting protocol, making them the dominant single-particle noise source for measuring $\langle \hat{S}^y \rangle$. The combination of cavity loss and spontaneous emission limits the metrological gain ξ^{-2} to [36],

$$\xi^2 \approx \frac{1 + 2N\Gamma_z t_0}{(N\chi t_0)^2} + \frac{8}{3}\gamma_r t_0, \tag{6}$$

leading to an optimal value $\xi^{-2}_{\mathrm{opt}} \propto \sqrt{NC'}$, where $C' = \chi^2/\Gamma_z\Gamma$ is related to the single-atom cooperativity [36]. This result translates into the sensitivity for gravimetry as $\Delta g/g \propto N^{-3/4}$ [see the blue curve in Fig. 4]. Higher sensitivity can be reached by choosing specific schemes (e.g., cycling transitions) to suppress spin flip processes [see the purple curve in Fig. 4].

Technical noise in experiment such as mechanical vibrations and local oscillator dephasing, as well as single particle decoherence due to interatomic interactions also impose a constraint on the interrogation time. In particular, single-particle decoherence imposes even more severe restrictions when operating with entangled states given their fragility to it [36]. For ^{87}Rb assuming a 5.32 μm atom separation achieved by $r = 5$, $m_R = 2$ in a $\lambda_l = 532$ nm lattice, phase accumulation time $\tau = 1$ s, $C' = 2$, and spin flip probability $P_f = 1/2$, one can achieve $\Delta g/g \sim 6 \times 10^{-9}/\sqrt{\mathrm{Hz}}$ with about 5×10^4 atoms, which is 20 dB enhancement beyond SQL. If we compare this sensitivity with SQL for $\tau = 10$ s, still a 10 dB enhancement is possible, meaning that even after accounting for the fragility of the spin squeezed states, our protocol can not only reduce the required averaging time by a factor of 10, but also increase the measurement bandwidth of the time-varying signal by a factor of 10, compared to unentangled lattice-based interferometers [12,20].

Conclusion and outlook.—We proposed a quantum enhanced interferometric protocol using Wannier-Stark states in standing-wave cavity QED system, which allows for homogeneous spin squeezing generation and micrometric spatial resolution for gravimetry and force sensing. The many-body entanglement in our scheme leads to an order of magnitude reduction of the required averaging time compared to unentangled lattice-based interferometers. Our work opens new possibilities for quantum enhanced interferometry in versatile compact atomic sensors, as well as novel Hamiltonian engineering in quantum many-body simulators.

We thank John Robinson, Colin Kennedy, Matthew Affolter, Graham Greve, Chengyi Luo, and Baochen Wu for useful discussions. This work is supported by the AFOSR Grant No. FA9550-18-1-0319, by the DARPA (funded via ARO) Grant No. W911NF-16-1-0576, the ARO single investigator Grant No. W911NF-19-1-0210, the NSF PHY1820885, NSF JILA-PFC PHY-1734006, and NSF QLCI-2016244 grants, by the DOE Quantum Systems Accelerator (QSA) grant and by NIST.

*anjun.chu@colorado.edu

[1] A. D. Ludlow, M. M. Boyd, J. Ye, E. Peik, and P. O. Schmidt, Rev. Mod. Phys. **87**, 637 (2015).
[2] G. M. Tino, Quantum Sci. Technol. **6**, 024014 (2021).
[3] M. Tse, H. Yu, N. Kijbunchoo, A. Fernandez-Galiana, P. Dupej, L. Barsotti, C. Blair, D. Brown, S. Dwyer, A. Effler *et al.*, Phys. Rev. Lett. **123**, 231107 (2019).
[4] F. Acernese, M. Agathos, L. Aiello, A. Allocca, A. Amato, S. Ansoldi, S. Antier, M. Arène, N. Arnaud, S. Ascenzi *et al.* (Virgo Collaboration), Phys. Rev. Lett. **123**, 231108 (2019).
[5] M. Malnou, D. A. Palken, B. M. Brubaker, L. R. Vale, G. C. Hilton, and K. W. Lehnert, Phys. Rev. X **9**, 021023 (2019).
[6] K. M. Backes, D. A. Palken, S. Al Kenany, B. M. Brubaker, S. B. Cahn, A. Droster, G. C. Hilton, S. Ghosh, H. Jackson, S. K. Lamoreaux *et al.*, Nature (London) **590**, 238 (2021).
[7] O. Hosten, N. J. Engelsen, R. Krishnakumar, and M. A. Kasevich, Nature (London) **529**, 505 (2016).
[8] K. C. Cox, G. P. Greve, J. M. Weiner, and J. K. Thompson, Phys. Rev. Lett. **116**, 093602 (2016).
[9] M. H. Schleier-Smith, I. D. Leroux, and V. Vuletić, Phys. Rev. Lett. **104**, 073604 (2010).
[10] E. Pedrozo-Peñafiel, S. Colombo, C. Shu, A. F. Adiyatullin, Z. Li, E. Mendez, B. Braverman, A. Kawasaki, D. Akamatsu, Y. Xiao, and V. Vuletić, Nature (London) **588**, 414 (2020).
[11] J. Hu, W. Chen, Z. Vendeiro, H. Zhang, and V. Vuletić, Phys. Rev. A **92**, 063816 (2015).
[12] X. Alauze, A. Bonnin, C. Solaro, and F. Pereira Dos Santos, New J. Phys. **20**, 083014 (2018).
[13] J. Lee, G. Vrijsen, I. Teper, O. Hosten, and M. A. Kasevich, Opt. Lett. **39**, 4005 (2014).
[14] Y. Wu, R. Krishnakumar, J. Martínez-Rincón, B. K. Malia, O. Hosten, and M. A. Kasevich, Phys. Rev. A **102**, 012224 (2020).
[15] S. Bernon, T. Vanderbruggen, R. Kohlhaas, A. Bertoldi, A. Landragin, and P. Bouyer, New J. Phys. **13**, 065021 (2011).
[16] L. Salvi, N. Poli, V. Vuletić, and G. M. Tino, Phys. Rev. Lett. **120**, 033601 (2018).
[17] A. Shankar, L. Salvi, M. L. Chiofalo, N. Poli, and M. J. Holland, Quantum Sci. Technol. **4**, 045010 (2019).
[18] K. Gietka, F. Mivehvar, and H. Ritsch, Phys. Rev. Lett. **122**, 190801 (2019).
[19] K. C. Cox, G. P. Greve, B. Wu, and J. K. Thompson, Phys. Rev. A **94**, 061601(R) (2016).
[20] M. G. Tarallo, T. Mazzoni, N. Poli, D. V. Sutyrin, X. Zhang, and G. M. Tino, Phys. Rev. Lett. **113**, 023005 (2014).
[21] H. Keßler, J. Klinder, B. P. Venkatesh, C. Georges, and A. Hemmerich, New J. Phys. **18**, 102001 (2016).
[22] V. Xu, M. Jaffe, C. D. Panda, S. L. Kristensen, L. W. Clark, and H. Müller, Science **366**, 745 (2019).

[23] L. Morel, Z. Yao, P. Cladé, and S. Guellati-Khélifa, Nature (London) **588**, 61 (2020).
[24] M. Kitagawa and M. Ueda, Phys. Rev. A **47**, 5138 (1993).
[25] D. J. Wineland, J. J. Bollinger, W. M. Itano, F. L. Moore, and D. J. Heinzen, Phys. Rev. A **46**, R6797 (1992).
[26] V. B. Braginsky and F. Y. Khalili, Rev. Mod. Phys. **68**, 1 (1996).
[27] A. Kuzmich, N. P. Bigelow, and L. Mandel, Europhys. Lett. **42**, 481 (1998).
[28] M. Jaffe, P. Haslinger, V. Xu, P. Hamilton, A. Upadhye, B. Elder, J. Khoury, and H. Müller, Nat. Phys. **13**, 938 (2017).
[29] D. M. Harber, J. M. Obrecht, J. M. McGuirk, and E. A. Cornell, Phys. Rev. A **72**, 033610 (2005).
[30] D. J. Kapner, T. S. Cook, E. G. Adelberger, J. H. Gundlach, B. R. Heckel, C. D. Hoyle, and H. E. Swanson, Phys. Rev. Lett. **98**, 021101 (2007).
[31] A. O. Sushkov, W. J. Kim, D. A. R. Dalvit, and S. K. Lamoreaux, Phys. Rev. Lett. **107**, 171101 (2011).
[32] H. Ritsch, P. Domokos, F. Brennecke, and T. Esslinger, Rev. Mod. Phys. **85**, 553 (2013).
[33] E. Davis, G. Bentsen, and M. Schleier-Smith, Phys. Rev. Lett. **116**, 053601 (2016).
[34] O. Hosten, R. Krishnakumar, N. J. Engelsen, and M. A. Kasevich, Science **352**, 1552 (2016).
[35] M. Schulte, V. J. Martínez-Lahuerta, M. S. Scharnagl, and K. Hammerer, Quantum **4**, 268 (2020).
[36] See Supplemental Material at http://link.aps.org/supplemental/10.1103/PhysRevLett.127.210401 for details of adiabatic elimination, model validity and experimental considerations, which includes Refs. [19,33,37–45].
[37] M. Glück, A. R. Kolovsky, and H. J. Korsch, Phys. Rep. **366**, 103 (2002).
[38] D. F. James and J. Jerke, Can. J. Phys. **85**, 625 (2007).
[39] C. Maschler and H. Ritsch, Phys. Rev. Lett. **95**, 260401 (2005).
[40] B. Prasanna Venkatesh, M. Trupke, E. A. Hinds, and D. H. J. O'Dell, Phys. Rev. A **80**, 063834 (2009).
[41] F. Reiter and A. S. Sørensen, Phys. Rev. A **85**, 032111 (2012).
[42] S. Kolkowitz, S. L. Bromley, T. Bothwell, M. L. Wall, G. E. Marti, A. P. Koller, X. Zhang, A. M. Rey, and J. Ye, Nature (London) **542**, 66 (2017).
[43] C.-G. Ji, Y.-C. Liu, and G.-R. Jin, Quantum Inf. Comput. **13**, 266 (2013).
[44] M. Foss-Feig, K. R. A. Hazzard, J. J. Bollinger, and A. M. Rey, Phys. Rev. A **87**, 042101 (2013).
[45] S. F. Huelga, C. Macchiavello, T. Pellizzari, A. K. Ekert, M. B. Plenio, and J. I. Cirac, Phys. Rev. Lett. **79**, 3865 (1997).
[46] V. A. Dzuba and A. Derevianko, J. Phys. B **43**, 074011 (2010).
[47] M. A. Cazalilla and A. M. Rey, Rep. Prog. Phys. **77**, 124401 (2014).
[48] B. Pelle, A. Hilico, G. Tackmann, Q. Beaufils, and F. Pereira Dos Santos, Phys. Rev. A **87**, 023601 (2013).